IN-64
61450
P-31

NASA Contractor Report 189578
ICASE Report No. 91-88

ICASE

APPROXIMATION METHODS FOR CONTROL OF ACOUSTIC/STRUCTURE MODELS WITH PIEZOCERAMIC ACTUATORS

H.T. Banks
W. Fang
R.J. Silcox
R.C. Smith

Contract No. NAS1-18605
December 1991

Institute for Computer Applications in Science and Engineering
NASA Langley Research Center
Hampton, Virginia 23665-5225

Operated by the Universities Space Research Association

National Aeronautics and
Space Administration

Langley Research Center
Hampton, Virginia 23665-5225

APPROXIMATION METHODS FOR CONTROL OF ACOUSTIC/STRUCTURE MODELS WITH PIEZOCERAMIC ACTUATORS [1]

H.T. Banks [2]
W. Fang [2]
R.J. Silcox [3]
R.C. Smith [4]

ABSTRACT

The active control of acoustic pressure in a 2-D cavity with a flexible boundary (a beam) is considered. Specifically, this control is implemented via piezoceramic patches on the beam which produce pure bending moments. The incorporation of the feedback control in this manner leads to a system with an unbounded input term. Approximation methods in the context of an LQR state space formulation are discussed and numerical results demonstrating the effectiveness of this approach in computing feedback controls for noise reduction are presented.

[1] Research supported in part (H.T.B & W.F.) by the Air Force Office of Scientific Research under grant AFOSR-90-0091 and NASA grant NAG-1-1116. This research was carried out in part while the first author was a visiting scientist at the Institute for Computer Applications in Science and Engineering (ICASE), NASA Langley Research Center, Hampton, VA 23666, which is operated under NASA Contract No. NAS1-18107.
[2] Center for Applied Mathematical Sciences, University of Southern California, LA, CA 90089
[3] Acoustic Division, NASA Langley Research Center, Hampton, VA 23665
[4] ICASE, NASA Langley Research Center, Hampton, VA 23665

1 Introduction

In recent years, the development of new fuel efficient turboprop engines has motivated the development of a comprehensive active control methodology for interior pressure field chambers. The active control of noise in this setting has been studied both in a frequency domain setting [14, 19] and from an infinite dimensional state space time domain approach (PDE approach) [2, 6, 7, 12] with techniques often centering around the generation of an appropriate secondary pressure wave which optimally interferes with the offending primary pressure wave. Here however, we consider a time domain state space formulation in which the active control is implemented via piezoceramic patches which are imbedded in the boundary of the acoustic cavity.

The example we consider consists of an exterior noise source which is separated from an interior chamber by an active wall or plate. This plate transmits noise or vibrations from the exterior field to the interior cavity via fluid/structure interactions thus leading to the formulation of a system of partial differential equations consisting of an acoustic wave equation coupled with elasticity equations for the plate. The control is implemented in the example via piezoceramic patches on the plate which are excited in a manner so as to produce pure bending moments. It should be noted that the incorporation of the feedback control in this manner leads to a system with an unbounded input term. Experiments are being designed and carried out at NASA Langley Research Center in which the interior cavity is taken to be cylindrical with a circular active plate and sectorial patches.

As a first step toward developing an effective linear quadratic regulator (LQR) state space control methodology for near field acoustic problems of this type, it is useful to consider a simplified but typical model consisting of a 2-D interior cavity with an active beam at one end (see Figure 1). Here $\mathcal{F}$ represents a perturbing force on the beam due to an exterior noise source. This in turn causes fluctuations in the interior acoustic pressure field and hence unwanted noise. The goal in the control problem is to optimally reduce the interior pressure deviations by effecting a force distribution on the beam that decouples the cavity acoustic response.

In Section 2, a model set of differential equations for the problem is given and the mathematical framework needed to pose the control system in an abstract Cauchy formulation is presented. Section 3 contains a brief discussion of the theory of finite and infinite dimensional periodic optimal control problems while Section 4 is devoted to the general finite dimensional approximation of the control problem. Specific approximation schemes are discussed in the fifth section and examples demonstrating the viability of the method are presented.

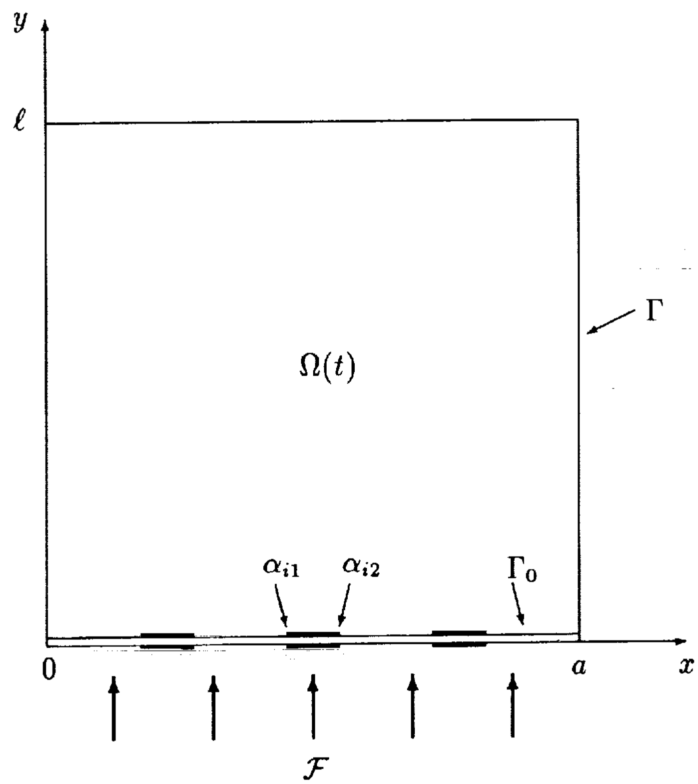

Figure 1. Acoustic chamber with piezoceramic patches.

2 Mathematical Model

When describing acoustic wave motion in a fluid, it is useful to introduce a velocity potential ϕ which is a complex-valued function satisfying $\vec{v}(t,x,y) = -\nabla\phi(t,x,y)$ where $\vec{v}$ denotes the fluid's velocity [15, 16]. If the equilibrium density of the fluid is given by ρ_f, the acoustic pressure p (the deviation from the mean pressure at equilibrium) is related to this velocity potential by $p(t,x,y) = \rho_f\phi_t(t,x,y)$. For acoustic waves with small amplitude, both the potential and the pressure satisfy the undamped first order wave equation with uniform speed of sound c in the fluid; hence

$$\phi_{tt} = c^2\Delta\phi \qquad (x,y) \in \Omega(t)\ , t > 0\ .$$

The boundaries on three sides of the variable cavity $\Omega(t)$ are taken to be "hard" walls thus leading to the zero normal velocity boundary conditions

$$\nabla\phi \cdot \hat{n} = 0 \qquad (x,y) \in \Gamma\ , t > 0$$

where $\hat{n}$ is the outer normal. It is assumed that the perturbable boundary consists of an impenetrable fixed-end Euler-Bernoulli beam with Kelvin-Voigt damping. If $w(t,x)$ is used to denote the transverse displacement of the beam with linear mass density ρ_b, the equations of motion are

$$
\begin{aligned}
&\rho_b w_{tt} + \frac{\partial^2}{\partial x^2} M(t,x) = -\rho_f \phi_t(t,x,w(t,x)) + f(t,x) \qquad && 0 < x < a \ , \ t > 0 \ , \\
&w(t,0) = \frac{\partial w}{\partial x}(t,0) = w(t,a) = \frac{\partial w}{\partial x}(t,a) = 0 \qquad t > 0 \ ,
\end{aligned}
\tag{2.1}
$$

where $M(t,x)$ is the internal moment and f is the external applied force due to pressure from the exterior noise field. For an uncontrolled beam with Kelvin-Voigt damping, the moment contains both strain and strain rate components and is given by

$$M(t,x) = EI\frac{\partial^2 w}{\partial x^2} + c_D I \frac{\partial^3 w}{\partial x^2 \partial t} \ .$$

The final coupling equation is the continuity of velocity condition

$$w_t(t,x) = \nabla\phi(t,x,w(t,x)) \cdot \hat{n} \ , \quad 0 < x < a \ , t > 0 \tag{2.2}$$

which results from the assumption that the beam is impenetrable to fluid. Under an assumption of small displacements ($w(t,x) = \hat{w}(t,x) + \delta$ where $\hat{w} \equiv 0$) which is inherent in the Euler-Bernoulli formulation, the beam equation in (2.1) can be approximated by

$$\rho_b w_{tt} + \frac{\partial^2}{\partial x^2} M(t,x) = -\rho_f[\phi_t(t,x,0) + \phi_{ty}(t,x,0)w] + f(t,x)$$

while (2.2) can be approximated by

$$w_t(t,x) = \nabla\phi(t,x,0) \cdot \hat{n} + (\nabla\phi_y(t,x,0)w) \cdot \hat{n} \ .$$

To first order, these last two equations can be approximated by dropping the higher order terms $-\rho_f\phi_{ty}(t,x,0)w$ and $(\nabla\phi_y(t,x,0)w) \cdot \hat{n}$. Then upon approximating the domain $\Omega(t)$ by the fixed domain $\Omega \equiv [0,a] \times [0,\ell]$, we obtain the approximate uncontrolled model

$$
\begin{aligned}
&\phi_{tt} = c^2 \Delta\phi \qquad (x,y) \in \Omega \ , t > 0 \ , \\
&\nabla\phi \cdot \hat{n} = 0 \qquad (x,y) \in \Gamma \ , t > 0 \ , \\
&\frac{\partial \phi}{\partial y}(t,x,0) = -w_t(t,x) \qquad 0 < x < a \ , t > 0 \ , \\
&\rho_b w_{tt} + \frac{\partial^2}{\partial x^2}\left(EI\frac{\partial^2 w}{\partial x^2} + c_D I \frac{\partial^3 w}{\partial x^2 \partial t}\right) = -\rho_f \phi_t(t,x,0) + f(t,x) \qquad 0 < x < a \ , \ t > 0 \ , \\
&w(t,0) = \frac{\partial w}{\partial x}(t,0) = w(t,a) = \frac{\partial w}{\partial x}(t,a) = 0 \qquad t > 0 \ , \\
&\phi(0,x,y) = \phi_0(x,y) \quad , \quad w(0,x) = w_0(x) \\
&\phi_t(0,x,y) = \phi_1(x,y) \quad , \quad w_t(0,x) = w_1(x) \ .
\end{aligned}
\tag{2.3}
$$

For control of structural vibrations and the acoustic pressure field in this model, s piezoceramic patches are attached to the beam as shown in Figure 1. These patches are excited in a manner so as to produce pure bending moments ([8, 9, 11]) (see Figure 2). If H is used to denote the Heaviside function, the model for the controlled beam can be written as

$$\begin{aligned}\rho_b w_{tt} &+ \frac{\partial^2}{\partial x^2}\left(EI\frac{\partial^2 w}{\partial x^2} + c_D I \frac{\partial^3 w}{\partial x^2 \partial t}\right) + \rho_f \phi_t(t,x,0) \\ &= \frac{\partial^2}{\partial x^2}\left(EI\frac{K^B k}{\mathcal{T}}\sum_{i=1}^{s} u_i(t)\left[H(x-\alpha_{i1}) - H(x-\alpha_{i2})\right]\right) + f(t,x) \ .\end{aligned} \tag{2.4}$$

Here $u_i(t)$ is the voltage applied to the i^{th} patch, K^B is a parameter which depends on the geometry and piezoceramic material properties, $\mathcal{T}$ is the patch thickness and k is a material constant (see [8, 9]). It should be noted that the incorporation of (2.4) into (2.3) leads to a system with an unbounded input term since it involves the second derivative of the Heaviside function.

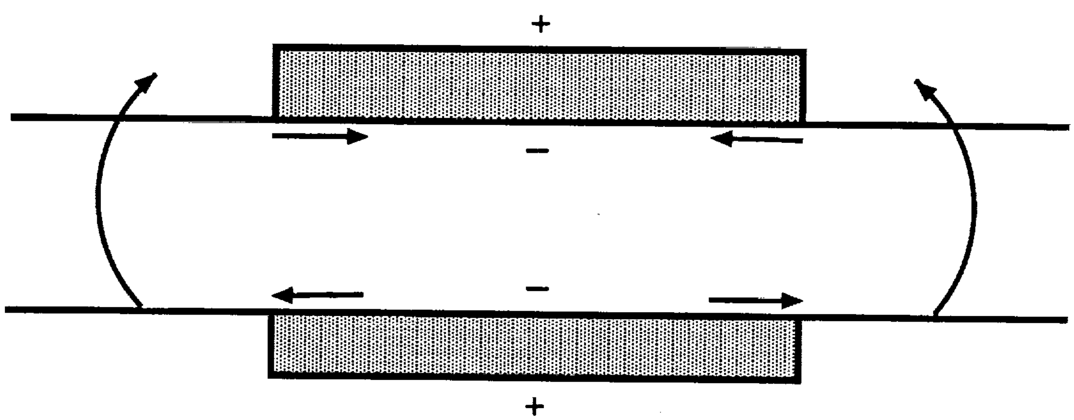

Figure 2. Piezoceramic patch excitation.

To formulate this problem in the context of existing infinite dimensional control theoretic results, it is advantageous to pose the control system in an abstract Cauchy formulation. To accomplish this, the state is taken to be $z = (\phi, w)$ in the Hilbert space $H = \bar{L}^2(\Omega) \times L^2(\Gamma_0)$ with the energy inner product

$$\left\langle \begin{pmatrix}\phi \\ w\end{pmatrix}, \begin{pmatrix}\xi \\ \eta\end{pmatrix}\right\rangle_H = \int_\Omega \frac{\rho_f}{c^2}\phi\xi d\omega + \int_{\Gamma_0}\rho_b w\eta d\gamma \ .$$

Here $\bar{L}^2(\Omega)$ is the quotient space of L^2 over the constant functions. We also define the Hilbert space $V = \bar{H}^1(\Omega) \times H_0^2(\Gamma_0)$ where $\bar{H}^1(\Omega)$ is the quotient space of H^1 over the constant functions and $H_0^2(\Gamma_0) = \{\psi \in H^2(\Gamma_0) : \psi(x) = \psi'(x) = 0 \text{ at } x = 0, a\}$. The V inner product is taken as (here and below we use the notation $D = \frac{\partial}{\partial x}$)

$$\left\langle \begin{pmatrix}\phi \\ w\end{pmatrix}, \begin{pmatrix}\xi \\ \eta\end{pmatrix}\right\rangle_V = \int_\Omega \nabla\phi\cdot\nabla\xi d\omega + \int_{\Gamma_0} D^2 w D^2 \eta d\gamma \ .$$

Following the ideas used in the theoretical results in [3, 4], we consider the Gelfand triple $V \hookrightarrow H \hookrightarrow V^*$ with pivot space H and define sesquilinear forms $\sigma_i : V \times V \to \mathbb{C}$, $i = 1,2$ by

$$\sigma_1(\Phi,\Psi) = \int_\Omega \rho_f \nabla\phi \cdot \nabla\xi d\omega + \int_{\Gamma_0} EID^2wD^2\eta d\gamma \ ,$$

$$\sigma_2(\Phi,\Psi) = \int_{\Gamma_0} \{c_D I D^2 w D^2\eta + \rho_f(\phi\eta - w\xi)\} d\gamma$$

where $\Phi = (\phi, w)$ and $\Psi = (\xi, \eta)$ are in V. It can be easily argued that the sesquilinear forms satisfy the continuity and coercivity conditions

$$\mathrm{Re}\ \sigma_1(\Phi,\Phi) \geq c_1|\Phi|_V^2 \ ,$$

$$|\sigma_1(\Phi,\Psi)| \leq c_2|\Phi|_V|\Psi|_V \ ,$$

$$\mathrm{Re}\ \sigma_2(\Phi,\Phi) \geq c_3 \left\langle D^2w, D^2w\right\rangle_{L^2(\Gamma_0)} = c_3|w|^2_{H_0^2(\Gamma_0)} \ ,$$

$$|\sigma_2(\Phi,\Psi)| \leq c_4|\Phi|_V|\Psi|_V$$

(for detailed arguments in a similar setting, see [1]). The control operator $B \in \mathcal{L}(U, V^*)$ is defined by

$$\langle Bu, \Psi\rangle_{V^*,V} = \int_{\Gamma_0} EI\frac{K^Bk}{\mathcal{T}}\sum_{i=1}^{s} u_i(H_{i1} - H_{i2})D^2\eta d\gamma$$

for $\Psi \in V$, where $H_{ij}(x) \equiv H(x - \alpha_{ij}), i = 1, 2, \cdots, s,\ j = 1,2$ and $\langle\cdot,\cdot\rangle_{V^*,V}$ is the usual duality pairing.

Finally, for $F = (0, f/\rho_b)$ we can write the control system in weak or variational form

$$\langle z_{tt}(t), \Psi\rangle_{V^*,V} + \sigma_2(z_t(t), \Psi) + \sigma_1(z(t), \Psi) = \langle Bu(t) + F, \Psi\rangle_{V^*,V} \tag{2.5}$$

for Ψ in V. The state is given by $z(t) = (\phi(t,\cdot,\cdot), w(t,\cdot))$ in $V \hookrightarrow H$. Since σ_1 and σ_2 are bounded, we can define operators $A_1, A_2 \in \mathcal{L}(V, V^*)$ by

$$\langle A_i\Phi, \Psi\rangle_{V^*,V} = \sigma_i(\Phi,\Psi)$$

for $i = 1,2$. This then yields the system

$$z_{tt}(t) + A_2 z_t(t) + A_1 z(t) = Bu(t) + F$$

in V^*.

Continuing with our abstract formulation, we next write the system in first order form. To accomplish this, define the product spaces $\mathcal{V} = V \times V$ and $\mathcal{H} = V \times H$ with the norms

$$|(\Phi,\Psi)|^2_{\mathcal{H}} = |\Phi|^2_V + |\Psi|^2_H$$

and

$$|(\Phi,\Psi)|^2_{\mathcal{V}} = |\Phi|^2_V + |\Psi|^2_V \ .$$

For $\chi = (\Phi, \Psi)$ and $\Theta = (\Upsilon, \Lambda)$, the sesquilinear form $\sigma : \mathcal{V} \times \mathcal{V} \to \mathbb{C}$ is then defined by

$$\sigma((\Upsilon,\Lambda),(\Phi,\Psi)) = -\langle\Lambda,\Phi\rangle_V + \sigma_1(\Upsilon,\Psi) + \sigma_2(\Lambda,\Psi) \ . \tag{2.6}$$

Since the duality product $\langle \cdot, \cdot \rangle_{V^*,V}$ is the unique extension by continuity of the scalar product $\langle \cdot, \cdot \rangle_H$ from $H \times V$ to $V^* \times V$, it follows that for appropriate restrictions on Θ we can write

$$\begin{aligned}
\sigma(\Theta, \chi) = \sigma((\Upsilon, \Lambda), (\Phi, \Psi)) &= -\langle \Lambda, \Phi \rangle_V + \langle A_1 \Upsilon, \Psi \rangle_{V^*,V} + \langle A_2 \Lambda, \Psi \rangle_{V^*,V} \\
&= -\langle \Lambda, \Phi \rangle_V + \langle A_1 \Upsilon + A_2 \Lambda, \Psi \rangle_H \\
&= \langle (-\Lambda, A_1 \Upsilon + A_2 \Lambda), (\Phi, \Psi) \rangle_{\mathcal{H}} \\
&= \langle -\mathcal{A}\Theta, \chi \rangle_{\mathcal{H}} .
\end{aligned}$$

The operator $\mathcal{A} : \mathcal{H} \to \mathcal{H}$ is given by

$$\mathcal{A} = \begin{bmatrix} 0 & I \\ -A_1 & -A_2 \end{bmatrix} \tag{2.7}$$

where $dom\ \mathcal{A} = \{\Theta = (\Upsilon, \Lambda) \in \mathcal{H} : \Lambda \in V, A_1\Upsilon + A_2\Lambda \in H\}$, A_1 and A_2 are the operators defined by σ_1 and σ_2, respectively, and the above calculations hold for $\Theta \in dom\ \mathcal{A}$ (see [1] for further examples concerning the definitions of operators and domains in this manner).

To write the first order system in weak or variational form, let $\mathcal{Z}(t) = (z(t), z_t(t))$, $\mathcal{F}(t) = (0, F(t))$, and $\mathcal{B}u(t) = (0, Bu(t))$. The weak form of the system is then

$$\langle \mathcal{Z}_t(t), \chi \rangle_{\mathcal{V}^*,\mathcal{V}} + \sigma(\mathcal{Z}(t), \chi) = \langle \mathcal{B}u(t) + \mathcal{F}(t), \chi \rangle_{\mathcal{V}^*,\mathcal{V}} \tag{2.8}$$

for $\chi \in \mathcal{V}$. Formally, this is equivalent to the system

$$\mathcal{Z}_t(t) = \mathcal{A}\mathcal{Z}(t) + \mathcal{B}u(t) + \mathcal{F}(t) \tag{2.9}$$

in $\mathcal{H}$ where $\mathcal{A}$ is given in (2.7).

3 Periodic Control Problems

As noted in the introduction, our control problem is motivated by the desire to reduce cavity pressure fluctuations resulting from the perturbing noise $\mathcal{F}$. In many applications, it is reasonable to assume that $\mathcal{F}$ is periodic with period τ; hence an important problem of interest (e.g., see [6]) for the system (2.9) is an LQR problem for a periodic disturbing force $\mathcal{F}$. This can be formulated as the problem of finding $u \in L^2(0, \tau; U)$ which minimizes a quadratic cost functional of the form

$$J(u) = \frac{1}{2} \int_0^\tau \{\langle \mathcal{Q}\mathcal{Z}(t), \mathcal{Z}(t) \rangle_{\mathcal{H}} + \langle Ru(t), u(t) \rangle_U\}\, dt$$

subject to (2.9) with $\mathcal{Z}(0) = \mathcal{Z}(\tau)$. Since $\mathcal{Z} = (\phi, w, \phi_t, w_t)^T$, the operator $\mathcal{Q}$ can be chosen so as to emphasize the minimization of particular state variables as well as to create windows that can be used to decrease state variations of certain frequencies. The control space U is taken to be $\mathbb{R}^s$ if s patches are used in the model, and it is assumed that the operator R is an $s \times s$ diagonal matrix where $r_{ii} > 0, i = 1, \cdots, s$ is the weight on the controlling voltage into the i^{th} patch. In the case that $\mathcal{B}$ is bounded on $\mathcal{H}$, a complete feedback theory for this problem can be given as discussed in [10]. Under usual stabilizability and detectability assumptions on the system as well as standard assumptions on $\mathcal{Q}$, the optimal control is given by

$$u(t) = -R^{-1}\mathcal{B}^*[\Pi\mathcal{Z}(t) - r(t)]$$

where Π is the unique nonnegative self-adjoint solution of the algebraic Riccati equation

$$\mathcal{A}^*\Pi + \Pi\mathcal{A} - \Pi\mathcal{B}R^{-1}\mathcal{B}^*\Pi + \mathcal{Q} = 0 \ . \tag{3.1}$$

Here r is the unique τ-periodic solution of

$$\dot{r}(t) + (\mathcal{A}^* - \Pi\mathcal{B}R^{-1}\mathcal{B}^*)r(t) - \Pi\mathcal{F}(t) = 0 \tag{3.2}$$

and the optimal trajectory $\mathcal{Z}$ is the solution of

$$\dot{\mathcal{Z}}(t) = (\mathcal{A} - \mathcal{B}R^{-1}\mathcal{B}^*\Pi)\mathcal{Z}(t) + \mathcal{B}R^{-1}\mathcal{B}^*r(t) + \mathcal{F}(t) \ .$$

These equations (in particular (3.1), (3.2)) are infinite dimensional (i.e., in $\mathcal{H}$) and hence approximation techniques are required to obtain approximate feedback gains. Using a standard Galerkin approach, one typically chooses a sequence of finite dimensional subspaces $\mathcal{H}^N \subset \mathcal{H}$ with projections $\mathcal{P}^N : \mathcal{H} \to \mathcal{H}^N$ and defines an approximating problem in $\mathcal{H}^N$ of minimizing

$$J^N(u) = \frac{1}{2}\int_0^\tau \left\{ \langle \mathcal{Q}^N\mathcal{Z}^N(t), \mathcal{Z}^N(t)\rangle_{\mathcal{H}} + \langle Ru(t), u(t)\rangle_U \right\} dt$$

subject to an approximating system

$$\begin{aligned} \dot{\mathcal{Z}}^N(t) &= \mathcal{A}^N\mathcal{Z}^N(t) + \mathcal{B}^N u(t) + \mathcal{F}^N(t) \\ \mathcal{Z}^N(0) &= \mathcal{Z}^N(\tau) = \mathcal{P}^N\mathcal{Z}(0). \end{aligned}$$

The solutions are given by

$$u^N(t) = -R^{-1}\mathcal{B}^{N*}[\Pi^N\mathcal{Z}^N(t) - r^N(t)]$$

$$\dot{\mathcal{Z}}^N(t) = (\mathcal{A}^N - \mathcal{B}^N R^{-1}\mathcal{B}^{N*}\Pi^N)\mathcal{Z}^N(t) + \mathcal{B}^N R^{-1}\mathcal{B}^{N*}r^N(t) + \mathcal{F}^N(t)$$

where Π^N is the unique nonnegative self-adjoint solution of

$$\mathcal{A}^{N*}\Pi^N + \Pi^N\mathcal{A}^N - \Pi^N\mathcal{B}^N R^{-1}\mathcal{B}^{N*}\Pi^N + \mathcal{Q}^N = 0$$

and r^N is the unique τ-periodic solution of

$$\dot{r}^N(t) + (\mathcal{A}^{N*} - \Pi^N\mathcal{B}^N R^{-1}\mathcal{B}^{N*})r^N(t) - \Pi^N\mathcal{F}^N(t) = 0.$$

In order to guarantee the convergence $\Pi^N\mathcal{P}^N\mathcal{Z} \to \Pi\mathcal{Z}$ for $\mathcal{Z} \in \mathcal{H}$, $r^N(t) \to r(t)$, and hence the convergence of $u^N(t)$ to $u(t)$, it is sufficient to impose various conditions on the original and approximation systems. These hypotheses include convergence requirements for the uncontrolled problem as well as the requirement that the approximation systems preserve stabilizability and detectability margins uniformly. A fully developed theory (see [4]) is available for the case that $\mathcal{F} \equiv 0$ (in this case the tracking variable r does not appear in the solution) even in the case that $\mathcal{B}$ is unbounded in the sense formulated in Section 1. The theory in [4] requires rather strong damping assumptions on the second order system (2.5) in order to be applicable. Under appropriate assumptions, the techniques and ideas of [3] and [4] can be used to treat the case for $\mathcal{F} \not\equiv 0$ in both identification and feedback control problems.

4 Finite Dimensional Approximation

An advantageous feature of the state space approach for feedback control is that the optimal control can be implemented using various approximation techniques. To illustrate the ideas involved, let $\{B_i^n\}_{i=1}^{n-1}$ denote the 1-D basis functions which are used to discretize the beam and let $\{B_i^m\}_{i=1}^{m}$, $m = (m_x+1)\cdot(m_y+1)-1$, denote the 2-D basis functions which are used in the cavity. The $n-1$ and m dimensional approximating subspaces are then taken to be $H_b^n = \text{span}\,\{B_i^n\}_{i=1}^{n-1}$ and $H_c^m = \text{span}\,\{B_i^m\}_{i=1}^{m}$, respectively. Defining $N = m+n-1$, the approximating state space is $H^N = H_c^m \times H_b^n$ and the product space for the first order system is $\mathcal{H}^N = H^N \times H^N$. The finite-dimensional approximation is then determined by restricting σ to $\mathcal{H}^N \times \mathcal{H}^N$ where σ is given in (2.6). This yields the operator $\mathcal{A}^N : \mathcal{H}^N \to \mathcal{H}^N$ where

$$\mathcal{A}^N = \begin{bmatrix} 0 & I \\ -A_1^N & -A_2^N \end{bmatrix}$$

and A_1^N and A_2^N are obtained by restricting σ_1 and σ_2 to $H^N \times H^N$. We observe that the restriction of the infinite dimensional system (2.5) to the space $\mathcal{H}^N \times \mathcal{H}^N$ yields for $\Psi = (\xi, \eta)$

$$\begin{aligned} \left\langle z_{tt}^N(t), \Psi \right\rangle_H &+ \sigma_2(z_t^N(t),\Psi) + \sigma_1(z^N(t),\Psi) \\ &= \int_{\Gamma_0} EI \frac{K^B k}{T} \sum_{i=1}^{s} u_i(t)\left(H_{i1} - H_{i2}\right) D^2\eta d\gamma + \int_{\Gamma_0} f\eta d\gamma \, . \end{aligned}$$

When Ψ is chosen in H^N and the approximate beam and cavity solutions are taken to be

$$w^N(t,x) = \sum_{i=1}^{n-1} w_i^N(t) B_i^n(x)$$

and

$$\phi^N(t,x,y) = \sum_{i=1}^{m} \phi_i^N(t) B_i^m(x,y) \, ,$$

respectively, this yields the system

$$M^N \dot{y}^N(t) = \tilde{A}^N y^N(t) + \tilde{B}^N u(t) + \tilde{F}^N(t)$$
$$M^N y^N(0) = \tilde{y}_0^N$$

where

$$y^N(t) = \begin{pmatrix} \vartheta^N(t) \\ \dot{\vartheta}^N(t) \end{pmatrix} .$$

Here $\vartheta^N(t) = (\phi_1^N(t), \phi_2^N(t), \cdots, \phi_m^N(t), w_1^N(t), w_2^N(t), \cdots, w_{n-1}^N(t))^T$ denotes the $N \times 1 = (m+n-1) \times 1$ approximate state vector coefficients while $u(t) = (u_1(t), \cdots u_s(t))^T$ contains the s control variables. The full system has the form

$$\begin{bmatrix} M_1^N & 0 \\ 0 & M_2^N \end{bmatrix} \begin{bmatrix} \dot{\vartheta}^N(t) \\ \ddot{\vartheta}^N(t) \end{bmatrix} = \begin{bmatrix} 0 & M_1^N \\ -A_1^N & -A_2^N \end{bmatrix} \begin{bmatrix} \vartheta^N(t) \\ \dot{\vartheta}^N(t) \end{bmatrix} + \begin{bmatrix} 0 \\ \tilde{B}^N \end{bmatrix} u(t) + \begin{bmatrix} 0 \\ \tilde{F}^N(t) \end{bmatrix}$$

$$\begin{bmatrix} M_1^N & 0 \\ 0 & M_2^N \end{bmatrix} \begin{bmatrix} \vartheta^N(0) \\ \dot{\vartheta}^N(0) \end{bmatrix} = \begin{bmatrix} g_1^N \\ g_2^N \end{bmatrix}$$

with

$$M_1^N = \mathrm{diag}[M_{11}^N, M_{12}^N] ,$$
$$M_2^N = \mathrm{diag}[M_{21}^N, M_{22}^N] ,$$
$$A_1^N = \mathrm{diag}[A_{11}^N, A_{12}^N] ,$$
$$A_2^N = \begin{bmatrix} 0 & A_{31}^N \\ A_{32}^N & A_{22}^N \end{bmatrix}$$

and

$$\tilde{B}^N = \begin{bmatrix} 0 & \cdots & 0 \\ \tilde{B}_{21}^N & \cdots & \tilde{B}_{2s}^N \end{bmatrix} ,$$

$$\tilde{F}^N(t) = \begin{bmatrix} 0 \\ \tilde{F}_2^N(t) \end{bmatrix} .$$

The component matrices are given by

$$\left[M_{11}^N\right]_{\ell,k} = \int_\Omega \nabla B_k^m \cdot \nabla B_\ell^m d\omega \ , \quad \left[M_{12}^N\right]_{p,i} = \int_{\Gamma_0} D^2 B_i^n D^2 B_p^n d\gamma \ ,$$

$$\left[M_{21}^N\right]_{\ell,k} = \int_\Omega \frac{\rho_f}{c^2} B_k^m B_\ell^m d\omega \ , \quad \left[M_{22}^N\right]_{p,i} = \int_{\Gamma_0} \rho_b B_i^n B_p^n d\gamma \ ,$$

$$\left[A_{11}^N\right]_{\ell,k} = \int_\Omega \rho_f \nabla B_k^m \cdot \nabla B_\ell^m d\omega \ , \quad \left[A_{12}^N\right]_{p,i} = \int_{\Gamma_0} EID^2 B_i^n D^2 B_p^n d\gamma \ ,$$

$$\left[A_{31}^N\right]_{\ell,i} = -\int_{\Gamma_0} \rho_f B_i^n B_\ell^m d\gamma \ , \quad \left[A_{32}^N\right]_{p,k} = \int_{\Gamma_0} \rho_f B_k^m B_p^n d\gamma \ ,$$

$$\left[A_{22}^N\right]_{p,i} = \int_{\Gamma_0} c_D I D^2 B_i^n D^2 B_p^n d\gamma \ ,$$

$$\left[\tilde{B}_2^N\right]_{p,j} = \int_{\alpha_{j1}}^{\alpha_{j2}} EI \frac{K^B k}{T} D^2 B_p^n d\gamma \ ,$$

$$\left[\tilde{F}_2^N(t)\right]_p = \int_{\Gamma_0} f B_p^n d\gamma \ .$$

Moreover, the vectors $g_1^N = \left[g_{11}^N, g_{12}^N\right]^T$ and $g_2^N = \left[g_{21}^N, g_{22}^N\right]^T$ have elements

$$\left[g_{11}^N\right]_\ell = \int_\Omega \nabla \phi_0 \cdot \nabla B_\ell^m d\omega \ , \quad \left[g_{12}^N\right]_p = \int_{\Gamma_0} D^2 w_0 D^2 B_p^n d\gamma \ ,$$

$$\left[g_{21}^N\right]_\ell = \int_\Omega \phi_1 B_\ell^m d\omega \ , \quad \left[g_{12}^N\right]_p = \int_{\Gamma_0} w_1 B_p^n d\gamma \ .$$

In all cases, the index ranges are $k, \ell = 1, \cdots, m$ and $i, p = 1, \cdots, n-1$. The patch index j ranges from 1 to s. It should be noted that the matrices A_1^N and M^N are symmetric and positive definite by construction. The matrix A_2^N has a symmetric block and a skewsymmetric block and the eigenvalues of A_2^N are real and nonnegative.

With the bases $\{B_i^n\}_{i=1}^{n-1}$ and $\{B_i^m\}_{i=1}^m$ chosen, the finite dimensional theory outlined in the last section holds with the various finite dimensional operators replaced by appropriate matrices. Specifically, the finite dimensional control problem is then to find $u \in L^2(0,\tau)$ which minimizes

$$J^N(u) = \frac{1}{2}\int_0^\tau \left\{ \langle Q^N y^N(t), y^N(t) \rangle_{\mathbf{R}^N} + \langle Ru(t), u(t) \rangle_{\mathbf{R}^s} \right\} dt \ , \quad N = m + n - 1$$

where Q^N is nonnegative definite and y^N solves

$$\begin{aligned} \dot{y}^N(t) &= A^N y^N(t) + B^N u(t) + F^N(t) \\ y^N(0) &= y_0^N \ . \end{aligned} \tag{4.1}$$

Here $A^N = \left(M^N\right)^{-1} \tilde{A}^N$, $B^N = \left(M^N\right)^{-1} \tilde{B}^N$, $F^N(t) = \left(M^N\right)^{-1} \tilde{F}^N(t)$ with the initial condition $y_0^N = \left(M^N\right)^{-1} \tilde{y}_0^N$. The optimal control is

$$u^N(t) = R^{-1}(B^N)^T \left[r^N(t) - \Pi^N y^N(t)\right] \tag{4.2}$$

where Π^N is the solution to the algebraic Riccati equation

$$(A^N)^T\Pi^N + \Pi^N A^N - \Pi^N B^N R^{-1}(B^N)^T\Pi^N + Q^N = 0 \ . \tag{4.3}$$

Since Q^N denotes the matrix representation for the operator $\mathcal{Q}^N$, a suitable choice for Q^N is

$$Q^N = \mathcal{D}\begin{bmatrix} M_1^N & 0 \\ 0 & M_2^N \end{bmatrix}$$

where the diagonal matrix $\mathcal{D}$ is given by

$$\mathcal{D} = \text{diag}\left[d_1 I^m, d_2 I^{n-1}, d_3 I^m, d_4 I^{n-1}\right] \ .$$

Here I^k , $k = m, n-1$, denotes a $k \times k$ identity and the parameters d_i are chosen to enhance stability and performance of the feedback. The $s \times s$ diagonal matrix R contains the positive control weights and has entries $r_{ii}, i = 1, \cdots, s$. For the regulator problem with periodic forcing function $F^N(t)$, $r^N(t)$ solves the linear differential equation

$$\begin{aligned} \dot{r}^N(t) &= -\left[A^N - B^N R^{-1}(B^N)^T\Pi^N\right]^T r^N(t) + \Pi^N F^N(t) \\ r^N(0) &= r^N(\tau) \end{aligned} \tag{4.4}$$

while the optimal trajectory is the solution to the linear differential equation

$$\begin{aligned} \dot{y}^N(t) &= \left[A^N - B^N R^{-1}(B^N)^T\Pi^N\right] y^N(t) + B^N R^{-1}(B^N)^T r^N(t) + F^N(t) \\ y^N(0) &= y^N(\tau) \ . \end{aligned} \tag{4.5}$$

5 Specific Approximations and Numerical Results

We next turn to a discussion of specific choices of basis functions in the general formulation of the approximation schemes in the last section. We shall also present numerical results from related computations. When choosing bases for the finite dimensional subspaces H_b^n and H_c^m in a control setting, one must weigh criteria such as smoothness requirements, uniform preservation of exponential stability of approximating systems (see [5]), accuracy, sparsity of system matrices and ease of implementation.

From energy considerations, it follows that the system (2.3) is dissipative; hence all the eigenvalues lie in the left half plane. The model of Section 1 includes no medium damping however, and hence the energy dissipation in the cavity results exclusively from the boundary (Kelvin-Voigt damping in the beam) thus making the system (2.3) only weakly damped. In spite of the lack of strong damping, numerical tests have indicated that when physically relevant parameters are used in the model, the system (2.3) is exponentially stable (the fixed-end boundary conditions on the beam make difficult a thorough analytical analysis of the eigenstructure). When considering various methods of discretizing the problem, one would like to choose schemes which uniformly preserve the exponential decay rate as the dimension of the approximate system (4.1) increases. This can be easily checked by determining whether or not there exists a uniform margin for increasing N between the open loop eigenvalues of the system matrix A^N in (4.1) and the imaginary axis.

When considering the control problem, one is also concerned with the preservation of uniform stabilizability and detectability margins for the closed loop approximation systems. Hence care must also be taken so that approximation schemes are chosen so as to preserve a uniform margin between the closed loop eigenvalues of $A^N - B^N R^{-1}(B^N)^T \Pi^N$ and the imaginary axis. Numerical schemes which satisfy these various criteria will now be discussed.

Cubic splines were used as a basis for H_b^n since they satisfy the smoothness requirement as well as being easily implemented when adapting to the fixed-end boundary conditions and patch discretizations. For a given positive integer n, a uniform partition was taken with the gridpoints $x_i^n = \frac{i}{n}a$, $i = 0, 1, \cdots, n$. If $\left\{\hat{B}_i^n\right\}_{i=-1}^{n+2}$ is used to denote the standard cubic spline basis corresponding to this partition (see [18], page 79), then the basis functions for the beam discretization were taken to be

$$\begin{aligned} B_1^n &= \hat{B}_0^n - 2\hat{B}_1^n - 2\hat{B}_{-1}^n \\ B_i^n &= \hat{B}_i^n \quad ; \; i = 2, 3, \cdots, n-2 \\ B_{n-1}^n &= \hat{B}_n^n - 2\hat{B}_{n-1}^n - 2\hat{B}_{n+1}^n \end{aligned}$$

It is readily seen that these basis functions satisfy the essential boundary conditions; that is,

$$B_i^n(0) = DB_i^n(0) = B_i^n(a) = DB_i^n(a) = 0$$

for $i = 1, 2, \cdots, n-1$. As mentioned previously, the corresponding $n-1$ dimensional approximating subspace is then given by $H_b^n = \text{span}\left\{B_i^n\right\}_{i=1}^{n-1}$ and the approximate beam solution is taken to be

$$w^N(t,x) = \sum_{i=1}^{n-1} w_i^N(t) B_i^n(x) \; .$$

With this choice of basis functions, the matrices M_{12}^N and M_{22}^N are easily constructed and are 7-banded. It should be noted that a Tau-Legendre discretization was also considered for the beam but had the disadvantage of the loss of four equations due to the constraints mandated by the fixed-end boundary conditions (see [13] for a discussion of Tau methods).

The bases that were considered for the cavity discretization included tensored one-dimensional Legendre polynomials, tensored linear splines and finite elements. The methods of system formulation as well as the advantages and disadvantages of each can be summarized as follows. Consider first the Legendre basis. Let $P_i^a(x)$ and $P_i^\ell(y)$ denote the standard Legendre polynomials that have been scaled by transformation to the intervals $[0, a]$ and $[0, \ell]$, respectively. The basis functions $\left\{B_{ij}^m\right\}$ for the cavity are then defined as

$$B_{ij}^m(x,y) = P_i^a(x) P_j^\ell(y) \quad \text{for} \quad i = 0, 1, \cdots, m_x, \;\; j = 0, 1, \cdots, m_y, \;\; i + j \neq 0,$$

where $m = (m_x + 1) \cdot (m_y + 1) - 1$. The condition $i + j \neq 0$ eliminates the constant function thus guaranteeing that the set of functions is suitable as a basis for the quotient space. For definiteness, the basis functions are ordered by assuming that i varies for each fixed j which is analogous to a left to right, bottom to top ordering. Notice that because natural boundary conditions occur on all sides of the cavity, one does not have to employ a Tau method; that is, the method is simply a Galerkin scheme without modification of the basis elements to satisfy some essential boundary conditions.

The component matrices M_{11}^N and M_{21}^N can then be succinctly described as follows. Let the fundamental $(m_x+1)\times(m_x+1)$ matrices M_a^m and K_a^m be defined as

$$[M_a^m]_{ij} = \int_0^a P_i^a(x)P_j^a(x)dx$$

$$[K_a^m]_{ij} = \int_0^a DP_i^a(x)DP_j^a(x)dx$$

with similar definitions for M_ℓ^m, K_ℓ^m. Using the tensor properties of the 2-D basis, we can form the matrices $\hat{M}_{11}^N$ and $\hat{M}_{21}^N$ defined by

$$\hat{M}_{11}^N = M_\ell^m \otimes K_a^m + K_\ell^m \otimes M_a^m$$

$$\hat{M}_{21}^N = \tfrac{\rho_f}{c^2} M_\ell^m \otimes M_a^m \quad .$$

The ordering in the above definition depends on the ordering of the basis functions. The matrices M_{11}^N and M_{21}^N are obtained by removing the first row and first column of $\hat{M}_{11}^N$ and $\hat{M}_{21}^N$ to reflect the deletion of the constant function from the basis set. Note that with this definition, both matrices are very easily constructed and that the mass matrix M_{21}^N is diagonal; hence the inverse is trivial to calculate. Although the matrix M_{11}^1 is not sparse, it has a well-defined structure due to its tensor product nature and the fact that M_a^m and M_l^m are diagonal. It too can be efficiently inverted when one takes advantage of this structure. In the case that ρ_f is constant, the stiffness matrix A_{11}^N can be constructed in the same manner as M_{11}^1 and the tensor product structure can be used advantageously both when solving the Riccati equation (4.3) and the ODE systems (4.4) and (4.5).

In order to use a tensored linear spline or finite element basis in the cavity, some constraint must be applied in order to guarantee that H_c^m is a quotient space (one cannot simply drop the constant function as was done with the tensored Legendre polynomials). One such constraint which is commonly used is the requirement that

$$\int_\Omega \phi^N(t,x,y)d\omega = 0 \ .$$

If $\left\{\tilde{B}_i^m\right\}_{i=1}^m$ is used to denote the standard tensor product linear spline basis (see page 129 of [18]), then the integral constraint leads to the quotient basis $\{B_i^m\}_{i=2}^m$ where

$$B_i^m(x,y) = \tilde{B}_i^m(x,y) - 4a_i\tilde{B}_1^m(x,y)$$

with $a_i = \left\{\frac{1}{4},\frac{1}{2},1\right\}$ depending upon whether the function B_i^m is a corner basis function, a side basis function or an interior basis function, respectively. As a result of the modifications needed to obtain a quotient space basis with the tensored linear splines, the matrices M_{11}^N, M_{12}^N and A_{11} are full and hence one loses the structural advantages obtained with the Legendre basis.

Similar modifications must be made when using a finite element basis in a quotient space with the result that the system matrices are also full in that case. Moreover, the lower order accuracy of the splines and finite elements necessitates the use of a larger number of basis functions and hence larger matrices in order to match the accuracy of the Legendre polynomials. The fact that the Legendre basis yields smaller, structured matrices than those obtained with the linear splines and finite elements is important but not crucial in the problem under consideration since the cavity is only two dimensional and hence matrix sizes are reasonably small. This issue will become much more critical when considering the 3-D problem of interest because of the large matrix sizes which will be encountered.

As discussed earlier, a final item which should be considered when choosing a means of discretizing the control problem is whether or not the approximation scheme effects a uniform preservation of exponential stability for the open and closed loop approximating systems. This issue is illustrated by the results in the Example 5.1.

The problem under consideration in Examples 5.1 and 5.2 is

$$
\begin{aligned}
&\phi_{tt} = c^2\Delta\phi \qquad (x,y)\in\Omega\ ,t>0\ ,\\
&\nabla\phi\cdot\hat{n} = 0 \qquad (x,y)\in\Gamma\ ,t>0\ ,\\
&\frac{\partial\phi}{\partial y}(t,x,0) = -w_t(t,x) \qquad 0<x<.6\ ,t>0\ ,\\
&\rho_b w_{tt} \;+\; \frac{\partial^2}{\partial x^2}\left(EI\frac{\partial^2 w}{\partial x^2} + c_D I\frac{\partial^3 w}{\partial x^2\partial t}\right)\\
&\qquad =\; \frac{\partial^2}{\partial x^2}\left(EI\frac{K^B k}{\mathcal{T}}u(t)\left[H(x-\alpha_{11}) - H(x-\alpha_{12})\right]\right)\\
&\qquad -\; \rho_f\phi_t(t,x,0) + f(t,x) \qquad 0<x<.6\ ,\ t>0\ ,\\
&w(t,0) = \frac{\partial w}{\partial x}(t,0) = w(t,.6) = \frac{\partial w}{\partial x}(t,.6) = 0 \qquad t>0\ ,\\
&\phi(0,x,y) = \phi_t(0,x,y) = w(0,x) = w_t(0,x) = 0
\end{aligned}
\tag{5.1}
$$

where

$$f(t,x) = 2.04\sin(150\pi t)\ .$$

The parameter choices $a = .6\ m$, $\ell = 1\ m$, $\rho_f = 1.21\ kg/m^3$, $c^2 = 117649\ m^2/sec^2$, $\rho_b = 1.35\ kg/m$, $EI = 73.96\ Nm^2$, $c_D I = .001\ kg\,m^3/sec$, $K^B = 82.9629$, $\mathcal{T} = .0005\ m$, $k = 1.9\times 10^{-10}\ m/V$, $\alpha_{i1} = .25$ and $\alpha_{i2} = .35$ are physically reasonable for a $.6\ m$ by $1\ m$ cavity in which the bounding end beam has a centered piezoceramic patch covering 1/6 of its length (see Figure 3). The beam is assumed to have width and thickness $.1\,m$ and $.005\,m$, respectively. The quadratic cost functional parameters were taken to be $d_1 = d_2 = d_4 = 1$, $d_3 = 10^4$ and $R = 10^{-6}$ with d_3 of much larger magnitude than d_1, d_2 or d_4 to emphasize the penalization of large pressure variations. Note that because there is only one patch, the control weight R is simply a positive scalar.

For a beam with the above dimensions and density, the natural frequency of the first mode is 73.21 hertz and the frequency of the forcing function was chosen so as to be close to this value. To obtain the magnitude 2.04, it was assumed that the forcing function was the result of an exterior plane wave with a sound pressure level of 120 dB (which forces an interior sound pressure level of 98 dB).

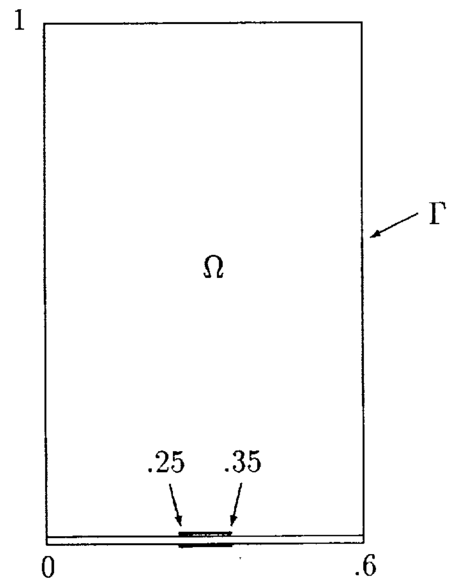

Figure 3. Example acoustic chamber with one piezoceramic patch.

Example 5.1

In this example, the uniform preservation of exponential stability for the open and closed loop approximating systems is examined. For $n = m_x = m_y = 5, 6, 7$ and 8, the margins of stability for the open and closed loop systems obtained with tensored Legendre polynomials and tensored linear splines are listed in Tables 1 and 2, respectively. The gains needed for the closed loop system were calculated via Potter's method (see [17]). For each n, the locations of the open and closed loop eigenvalues obtained with the Legendre polynomials are displayed in figures 4 and 5, respectively. When plotting the eigenvalues of A^N and $A^N - B^N R^{-1} \left(B^N\right)^T \Pi^N$, those eigenvalues having real parts with magnitude greater than 1 have been excluded in order to better see the distribution near the imaginary axis. Note that a uniform margin of stability is maintained between both the open and closed loop eigenvalues and the imaginary axis for both sets of bases. Results similar to those obtained with the Legendre basis were obtained when finite elements were used as a basis for H_c^m.

Table 1. Margin between the open and closed loop eigenvalues and the imaginary axis with tensored Legendre polynomials.

$m_x = m_y$	n	$\max\left\{Re\lambda, \lambda \in \sigma(A^N)\right\}$	$\max\left\{Re\lambda, \lambda \in \sigma\left(A^N - B^N R^{-1}\left(B^N\right)^T \Pi^N\right)\right\}$
5	5	$-.0145$	$-.0196$
6	6	$-.0213$	$-.0220$
7	7	$-.0200$	$-.0200$
8	8	$-.0158$	$-.0290$

Table 2. Margin between the open and closed loop eigenvalues and the imaginary axis with tensored linear splines.

$m_x = m_y$	n	$\max\left\{Re\lambda, \lambda \in \sigma(A^N)\right\}$	$\max\left\{Re\lambda, \lambda \in \sigma\left(A^N - B^N R^{-1}\left(B^N\right)^T \Pi^N\right)\right\}$
5	5	$-.0269$	$-.0868$
6	6	$-.0612$	$-.0612$
7	7	$-.1222$	$-.2732$
8	8	$-.2361$	$-.2388$

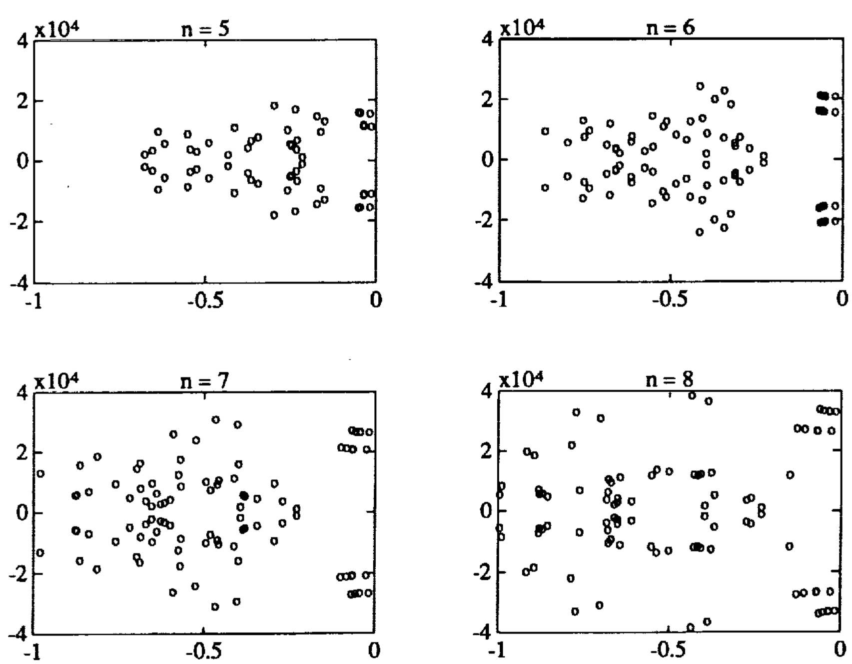

Figure 4. Eigenvalues of A^N for $n = m_x = m_y = 5, 6, 7$ and 8 with tensored Legendre polynomials.

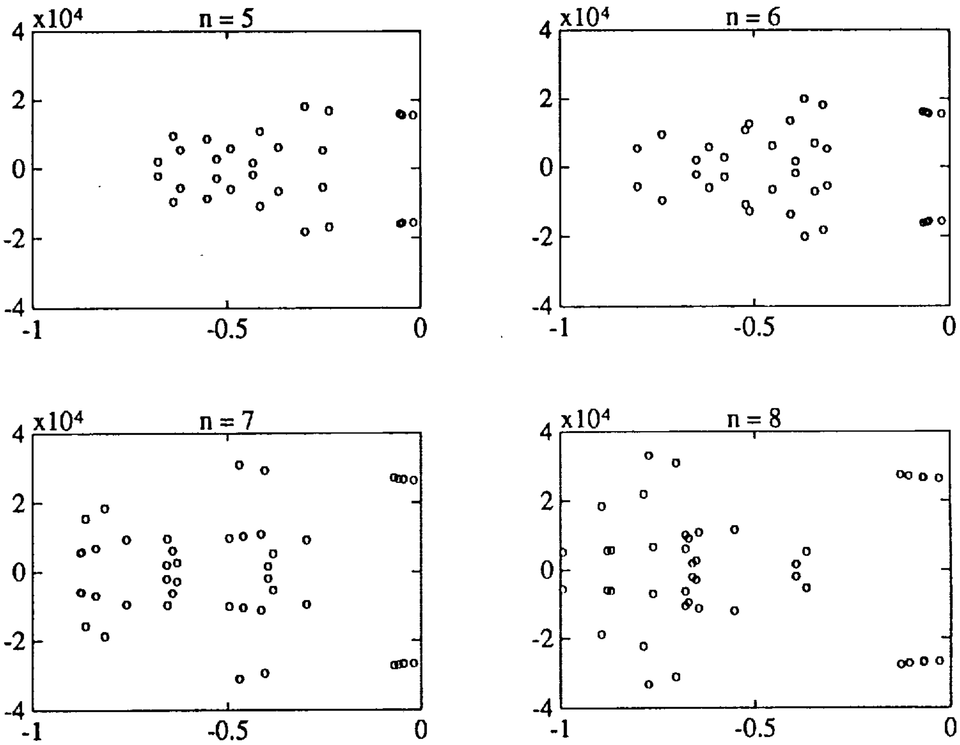

Figure 5. Eigenvalues of $\left[A^N - B^N R^{-1} \left(B^N\right)^T \Pi^N\right]$ for $n = m_x = m_y = 5, 6, 7$ and 8 with tensored Legendre polynomials.

As seen in Example 5.1, a larger margin of stability is maintained in both the open and closed loop systems with the linear spline basis than with the Legendre basis; hence one might conclude that the linear splines are the basis of choice when solving the control problem. As noted earlier however, one must also weigh factors such as system size, accuracy and efficiency when choosing a numerical method. Numerical tests have indicated that in spite of the larger eigenvalue margins of the linear splines, their performance when used in the control problem is nearly identical to that obtained with the Legendre polynomials. Moreover, because of the lower order accuracy of the splines, a larger number of basis functions is needed to obtain suitable accuracy thus leading to matrix dimensions that are almost twice those resulting from the Legendre discretization. Finally, as noted earlier in this section, the matrices obtained with the Legendre discretization are much more structured than those obtained with finite elements or linear splines hence making Legendre implementation more efficient than the other cases. Results for the LQR control problem for (5.1) with the tensored Legendre basis for the cavity and cubic splines for the beam with $m_x = m_y = 4$ and $n = 8$ are reported in Example 5.2.

Example 5.2

In this example, the effect of the feedback control on the problem for system (5.1) is described. In order to solve for the optimal control and trajectory, it is necessary to solve both the trajectory equation (4.5) and the tracking equation (4.4). Because numerical evidence indicated that both unconstrained solutions were roughly periodic with period $\tau = 1/75$, the problems were solved as initial value problems with starting values $y(0) = 0$ and $r(10/75) = 0$ rather than as free boundary value problems. The choice for initial state is physically reasonable while the choice to integrate backwards in time in (4.4) is made to reduce numerical instability when solving the ODE system for $r^N(t)$.

The uncontrolled and controlled approximate acoustic pressures ($p^N = \rho_f \phi_t^N$) at the point $(X, Y) = (.3, .1)$ are plotted in Figure 6 for the time interval $[0, 10/75]$. Similar plots for the approximate beam displacement at $X = .3$ are given in Figure 7. The uncontrolled solutions exhibit a beat phenomenon which results from the fact that the frequency of the forcing function is slightly greater than the natural frequency of the first mode of the beam. After a transient interval, the controlled solutions are periodic and are maintained at a level which is approximately 10% of that found in the uncontrolled case (note the scales in Figures 6 and 7). This produces an interior sound pressure level of 77 dB which is a 21 dB reduction. To further illustrate the state reduction with feedback control, the uncontrolled and controlled acoustic pressures at the times $T = 1/75$, $2/75$, $6/75$ and $10/75$ are plotted in Figures 8 - 11, respectively. The two dimensional plots in each figure show spatial slices of the uncontrolled and controlled pressures at $X = .3$, $0 \leq y \leq 1$. Figures 12 and 13 contain plots of the uncontrolled and controlled beam displacements at the times $T = 6/75$ and $T = 10/75$, respectively. The results in Figures 8 - 13 are representative of those found throughout the time interval $(0, 10/75]$ and in conjunction with Figures 6 and 7, demonstrate that the pressure and beam displacement are uniformly reduced and maintained at a very low level of magnitude in spite of the periodic forcing function.

The controlling voltage $u(t)$ is plotted in Figure 14. As expected, it is periodic with period 1/75. It should be noted that the magnitude of $u(t)$ remains less than $60V$ which is a physically reasonable voltage to put into the piezoceramic patches.

As mentioned in the last section, the choice of the quadratic cost functional parameters $d_1 - d_4$ and R influences the control stability and performance of the feedback. In this problem, the emphasis is on the the reduction of variations in the acoustic pressure; hence d_3 was taken to be larger than d_1, d_2 or d_4. It should be noted that this choice of parameters does not exclude the control of the other state variables; in fact, the beam displacement is significantly reduced as seen in Figures 7, 12 and 13. Since the parameter R is a penalty term for $u(t)$, more control of the state variables can be effected by choosing R smaller. The tradeoff, however, is an increase in the voltage. Hence one must weigh the amount of state reduction desired against the amount of voltage which can be put into the patches.

The amount of control is also directly influenced by patch size, placement and the number of patches being used. In the examples that we have observed, the best results were obtained with one centered patch, and we have noticed that the amount of control obtained increases with increasing patch length. Thus one must weigh the amount of control desired against physical limitations on the size of the piezoceramic patches being used.

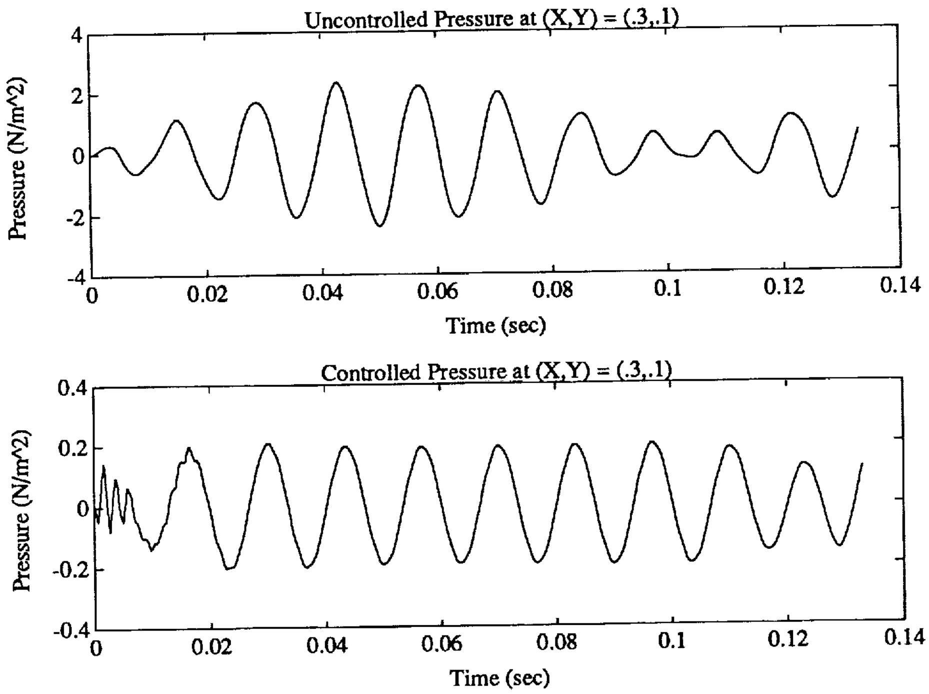

Figure 6. Uncontrolled and controlled pressures at the point $(X, Y) = (.3, .1)$ throughout the time interval $[0, 10/75]$.

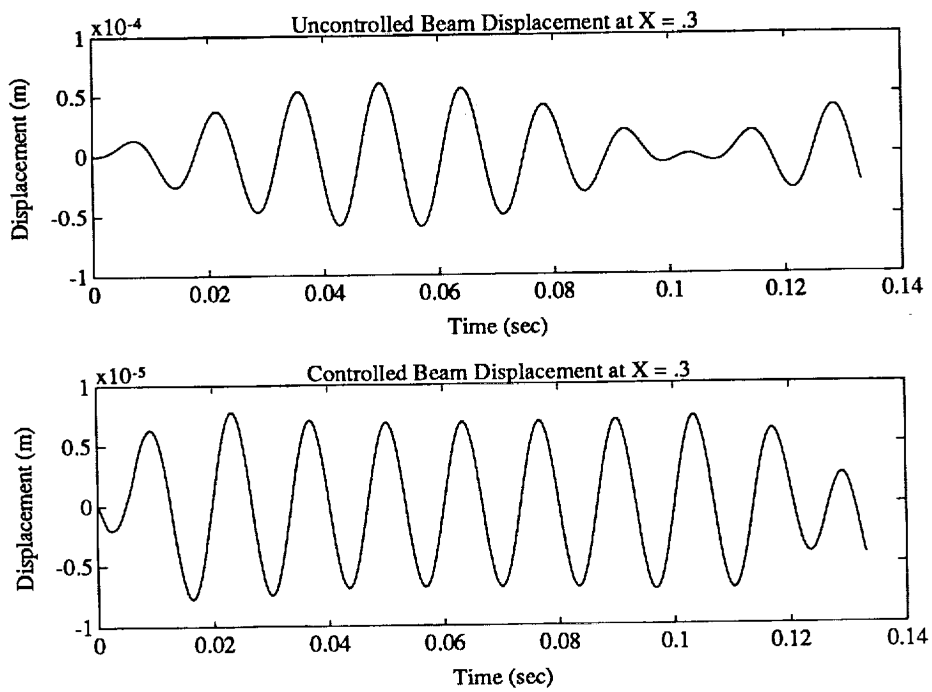

Figure 7. Uncontrolled and controlled beam displacements at the point $X = .3$ throughout the time interval $[0, 10/75]$.

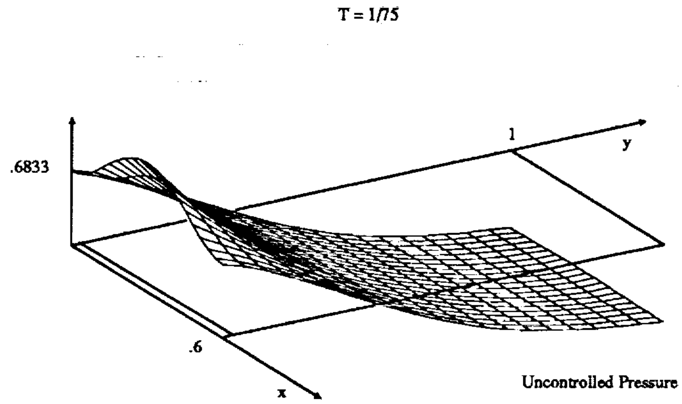

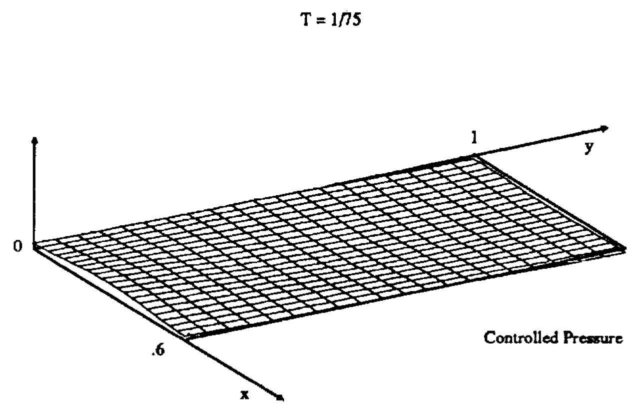

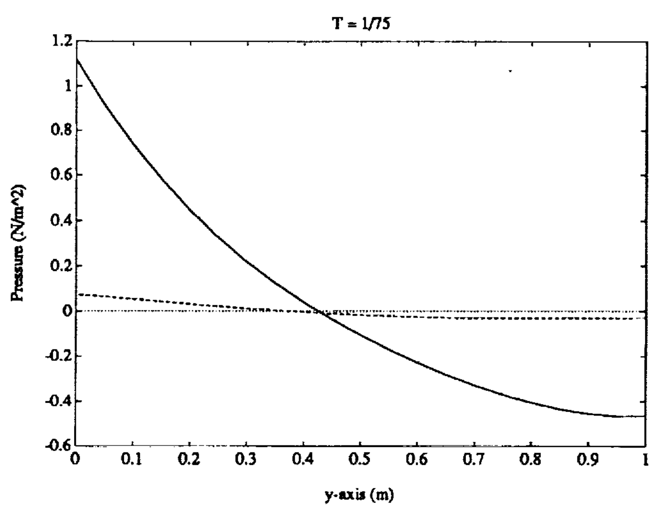

Figure 8. Uncontrolled and controlled pressures at $T = 1/75$, —— uncontrolled pressure, – – – controlled pressure.

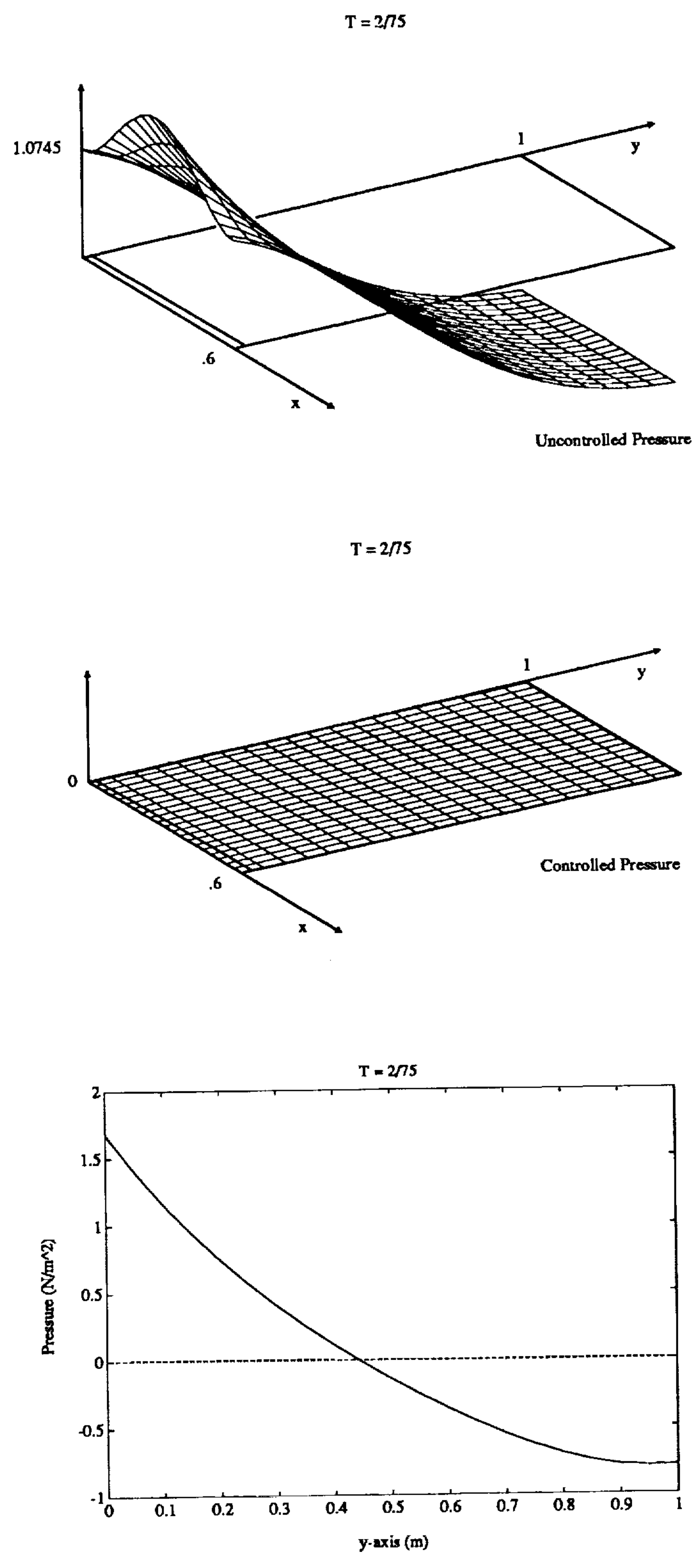

Figure 9. Uncontrolled and controlled pressures at $T = 2/75$, —— uncontrolled pressure, – – – controlled pressure.

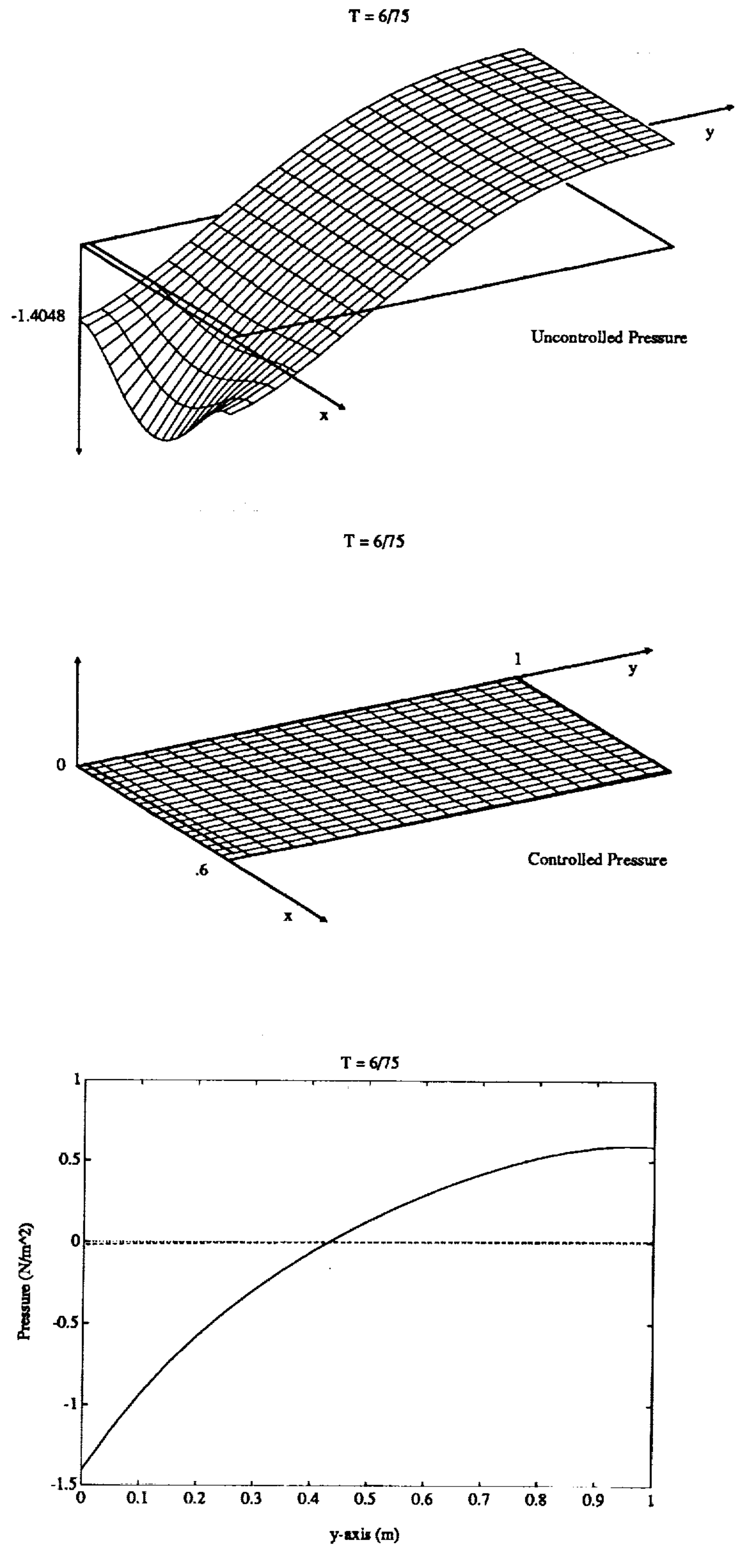

Figure 10. Uncontrolled and controlled pressures at $T = 6/75$, —— uncontrolled pressure, – – – controlled pressure.

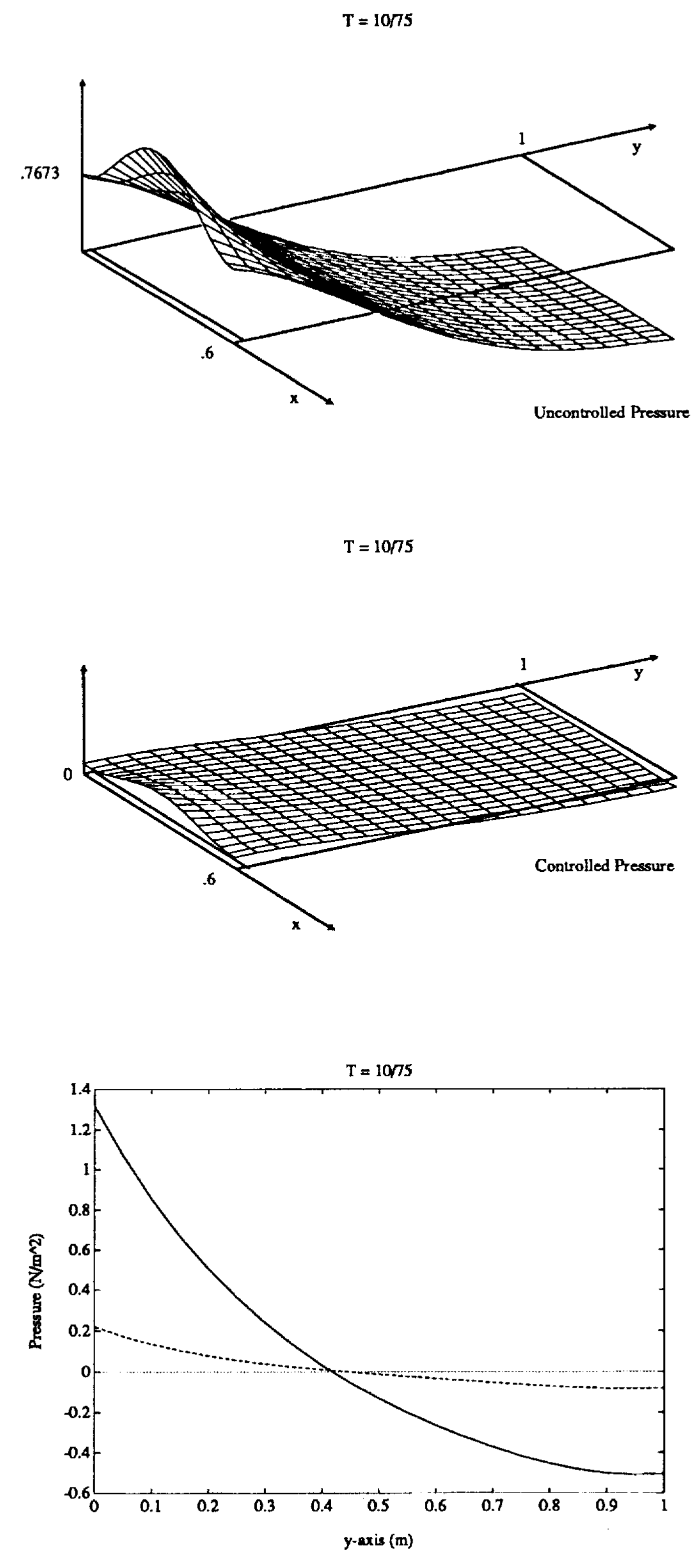

Figure 11. Uncontrolled and controlled pressures at $T = 10/75$ —— uncontrolled pressure, - - - controlled pressure.

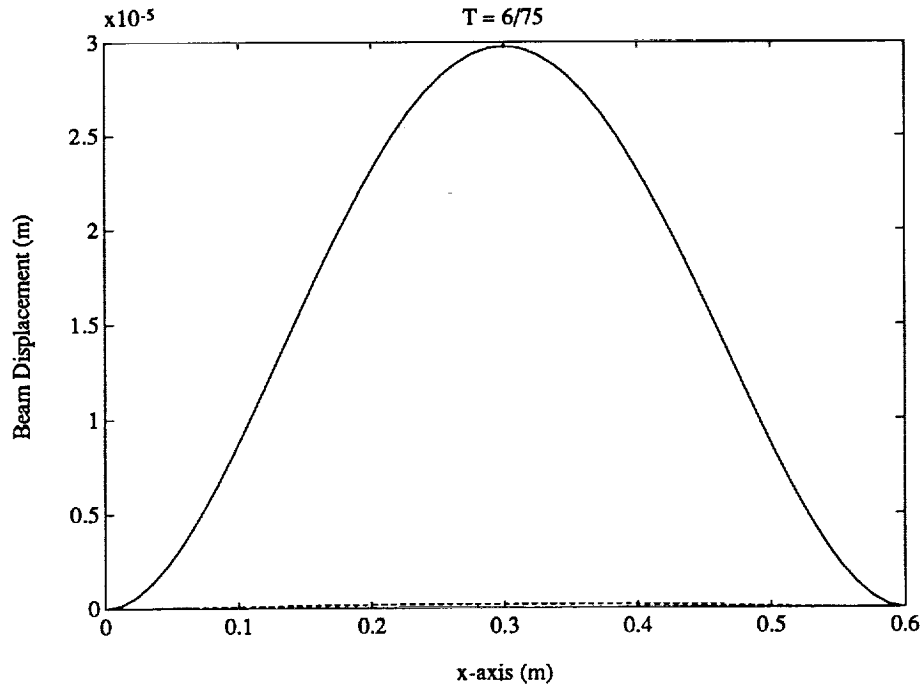

Figure 12. Uncontrolled and controlled beam displacements at $T = 6/75$ —— uncontrolled displacement, - - - controlled displacement.

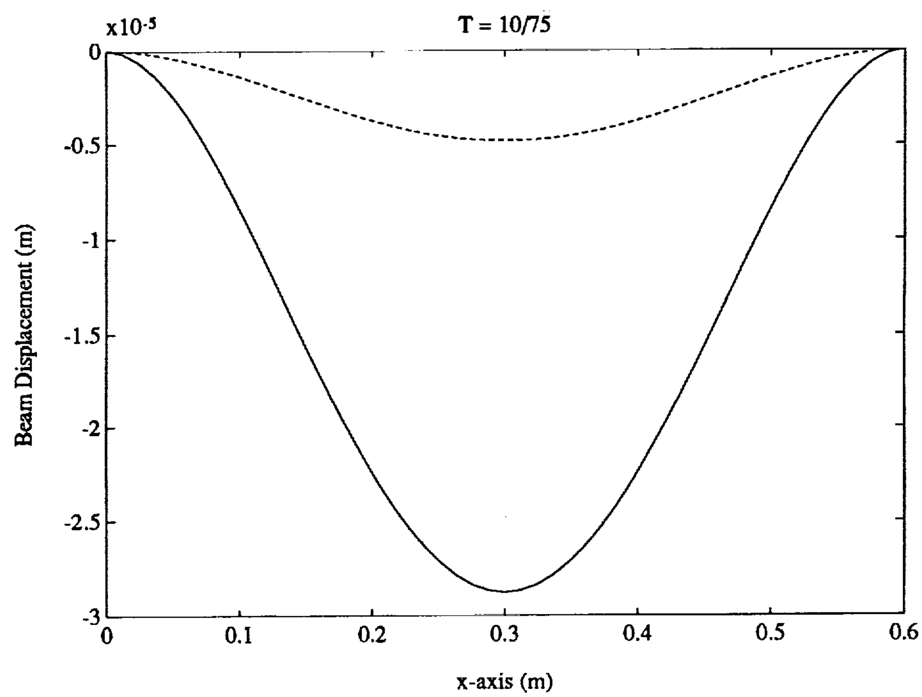

Figure 13. Uncontrolled and controlled beam displacements at $T = 10/75$ —— uncontrolled displacement, - - - controlled displacement.

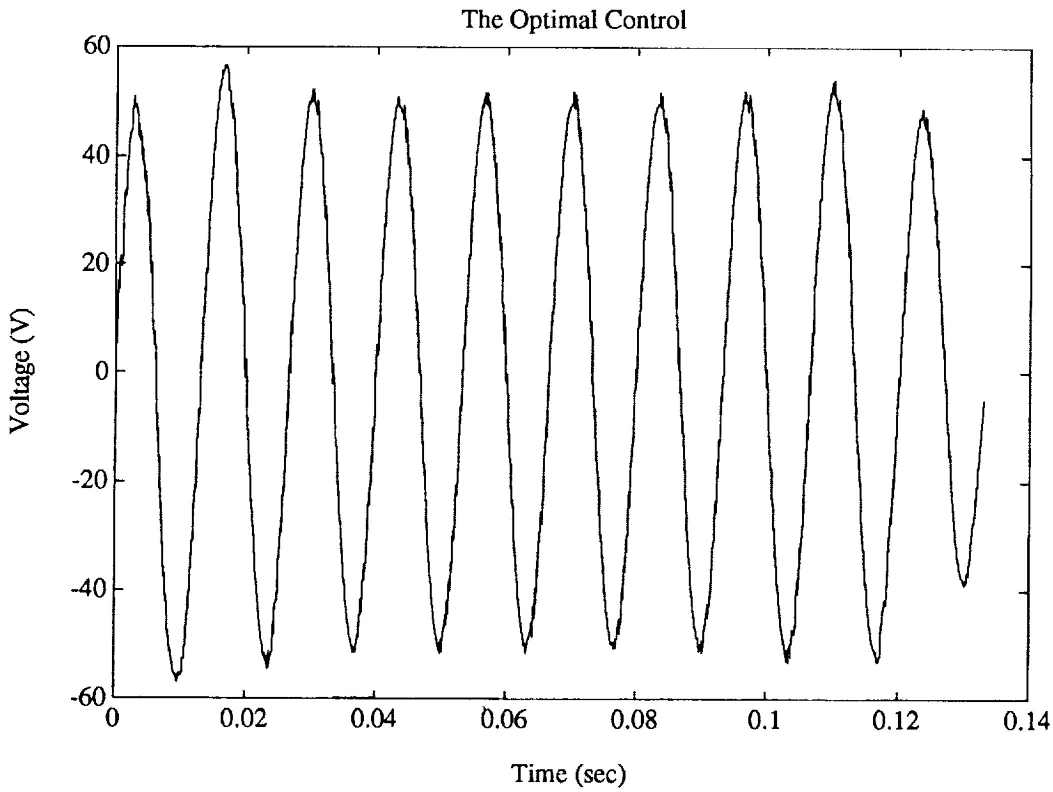

Figure 14. The optimal control $u(t)$.

6 Conclusion

For the 2-D acoustic problem involving the transmission of exterior noise into an interior cavity via fluid/structure interactions, a model set of differential equations has been developed. Control is implemented in the model via piezoceramic patches on the beam which are excited in a manner so as to produce pure bending moments. By writing the resulting system as an abstract Cauchy equation, the problem of reducing interior pressure fluctuations can be posed in the context of an LQR time domain state space formulation and approximation schemes which are suitable for this theory are presented.

For one typical patch configuration, examples are given which demonstrate the stabilizability of the open and closed loop systems under approximation as well as the reduction of cavity pressure and beam displacement when the feedback control is invoked. The examples show that input of the optimally controlling voltage $u(t)$ uniformly reduces both the pressure and the beam displacement and maintains them at a very low level of magnitude throughout the time interval of interest.

As mentioned in the example section, the amount of control obtained is directly influenced by patch size, placement and the number of patches being used. Initial results have indicated that for a uniform periodic forcing function, the best results can be obtained with one centered patch with the amount of control increasing with increasing patch length. Further computational studies are currently being conducted to determine the effect of various patch configurations and forcing functions on the decibel reduction in the cavity.

ACKNOWLEDGEMENT: The authors would like to express their sincere appreciation to H.C. Lester of the Acoustics Division, NASA Langley Research Center, for numerous discussions concerning the modeling of the acoustic problem.

References

[1] H.T. Banks and J.A. Burns, *Introduction to Control of Distributed Parameter Systems,* Birkhäuser, to appear.

[2] H.T. Banks, W. Fang and R.J. Silcox, Active control of noise: A time domain approach, *Proc. Conf. on Recent Advances in Active Control of Sound and Vibration*, (April 1991, VPISU), S43-S47.

[3] H.T. Banks and K. Ito, A unified framework for approximation in inverse problems for distributed parameter systems, Control-Theory and Advanced Technology, **4** (1988), 73-90.

[4] H.T. Banks and K. Ito, Approximation in LQR problems for infinite dimensional systems with unbounded input operators, *Proc. Conf. on Optimization*, Haifa, 1992, to appear.

[5] H.T. Banks, K. Ito and C. Wang, Exponentially stable approximations of weakly damped wave equations, CAMS Rep. 91-12, May, 1991, University of Southern California; in *DPS Control and Applications*, Birkhäuser, to appear.

[6] H.T. Banks, S.L. Keeling, and R.J. Silcox, Optimal control techniques for active noise suppression, *Proc. 27th IEEE Conf. on Decision and Control,* Austin, Texas, 1988, 2006-2011.

[7] H.T. Banks, S.L. Keeling, and C. Wang, Linear quadratic tracking problems in infinite dimensional Hilbert spaces and a finite dimensional approximation framework, LCDC/CCS Rep. 88-28, October, 1988, Brown University.

[8] R.L. Clark, Jr., C.R. Fuller and A. Wicks, Characterization of multiple piezoelectric actuators for structural excitation, J. Acoust. Soc. Amer., 1991, to appear.

[9] E.F. Crawley and E.H. Anderson, Detailed models of piezoceramic actuation of beams, AIAA Conf. Paper 89-1388-CP, 1989, 2000-2010.

[10] G. Da Prato, Synthesis of optimal control for an infinite dimensional periodic problem, SIAM J. Control Opt., **25** (1987), 706-714.

[11] E.K. Dimitriadis, C.R. Fuller and C.A. Rogers, Piezoelectric actuators for distributed noise and vibration excitation of thin plates, *Proc. 8th ASME Conf. on Failure, Prevention, Reliability and Stress Analysis*, Montreal, 1989, 223-233.

[12] F. Fakhroo, Legendre-Tau Approximation for an Active Noise Control Problem, Ph.D. Thesis, May, 1991, Brown University, Providence, RI.

[13] D. Gottlieb and S.A. Orszag, *Numerical Analysis of Spectral Methods: Theory and Applications*, SIAM, Philadelphia, 1977.

[14] H.C. Lester and C.R. Fuller, Active control of propeller induced noise fields inside a flexible cylinder, AIAA Tenth Aeroacoustics Conference, Seattle, WA, 1986.

[15] I. Malecki, *Physical Foundations of Technical Acoustics*, Translated by I. Bellert, Pergamon Press, New York, 1969.

[16] P.M. Morse and K.U. Ingard, *Theoretical Acoustics*, McGraw-Hill, New York, 1968.

[17] J.E. Potter, Matrix Quadratic Solutions, SIAM J. Appl. Math., **14** (1966), 496-501.

[18] P.M. Prenter, *Splines and Variational Methods*, Wiley Classics Edition, New York, 1989.

[19] R.J. Silcox, H.C. Lester and S.B. Abler, An Evaluation of Active Noise Control in a Cylindrical Shell, NASA Technical Memorandum 89090, February 1987.

REPORT DOCUMENTATION PAGE

Form Approved OMB No. 0704-0188

1. AGENCY USE ONLY (*Leave blank*)	2. REPORT DATE	3. REPORT TYPE AND DATES COVERED
	December 1991	Contractor Report

4. TITLE AND SUBTITLE

APPROXIMATION METHODS FOR CONTROL OF ACOUSTIC/STRUCTURE MODELS WITH PIEZOCERAMIC ACTUATORS

5. FUNDING NUMBERS

C NAS1-18605

WU 505-90-52-01

6. AUTHOR(S)

H.T. Banks, W. Fang, R.J. Silcox and R.C. Smith

7. PERFORMING ORGANIZATION NAME(S) AND ADDRESS(ES)

Institute for Computer Applications in Science and Engineering
Mail Stop 132C, NASA Langley Research Center
Hampton, VA 23665-5225

8. PERFORMING ORGANIZATION REPORT NUMBER

ICASE Report No. 91-88

9. SPONSORING/MONITORING AGENCY NAME(S) AND ADDRESS(ES)

National Aeronautics and Space Administration
Langley Research Center
Hampton, VA 23665-5225

10. SPONSORING/MONITORING AGENCY REPORT NUMBER

NASA CR-189578
ICASE Report No. 91-88

11. SUPPLEMENTARY NOTES

Langley Technical Monitor: Michael F. Card
Final Report

Submitted to Journal of Intelligent Material Systems and Structures.

12a. DISTRIBUTION/AVAILABILITY STATEMENT

Unclassified - Unlimited

Subject Category 64, 66

12b. DISTRIBUTION CODE

13. ABSTRACT (*Maximum 200 words*)

The active control of acoustic pressure in a 2-D cavity with a flexible boundary (a beam) is considered. Specifically, this control is implemented via piezoceramic patches on the beam which produce pure bending moments. The incorporation of the feedback control in this manner leads to a system with an unbounded input term. Approximation methods in the context of an LQR state space formulation are discussed and numerical results demonstrating the effectiveness of this approach in computing feedback controls for noise reduction are presented.

14. SUBJECT TERMS

LQR state space control; Acoustic/structure models; Piezoceramic Actuators

15. NUMBER OF PAGES 30

16. PRICE CODE A03

17. SECURITY CLASSIFICATION OF REPORT	18. SECURITY CLASSIFICATION OF THIS PAGE	19. SECURITY CLASSIFICATION OF ABSTRACT	20. LIMITATION OF ABSTRACT
Unclassified	Unclassified		

NSN 7540-01-280-5500

Standard Form 298 (Rev. 2-89)
Prescribed by ANSI Std. Z39-18
298-102